Journal of Colloid and Interface Science 331 (2009) 439–445

Contents lists available at ScienceDirect

Journal of Colloid and Interface Science

www.elsevier.com/locate/jcis

# Synthesis and characterization of arsenate-intercalated layered double hydroxides (LDHs): Prospects for arsenic mineralization

S.V. Prasanna, P. Vishnu Kamath *

*Department of Chemistry, Central College, Bangalore University, Bangalore 560 001, India*

ARTICLE INFO

*Article history:*
Received 4 October 2008
Accepted 22 November 2008
Available online 9 January 2009

*Keywords:*
Arsenic
Layered double hydroxides
Reversible thermal behavior
Arsenate exchange

ABSTRACT

The arsenate-intercalated layered double hydroxide (LDH) of Mg and Al is synthesized by coprecipitation. The higher thermodynamic stability and the consequent lower solubility of the unitary arsenates preclude the formation of arsenate-intercalated LDHs of other metals directly from solution. However other M/Al-$AsO_4$ (M = Co, Ni, Zn) LDHs could be prepared by anion exchange, showing that arsenate intercalation proceeds topotactically. The intercalation of various species of As(V) into the interlayer of LDHs and the subsequent arsenate carrying capacity are dependent upon the pH of the solution. Upon thermal decomposition, the intercalated arsenate ion undergoes reductive deintercalation to give a mixture of As(III) and As(V) oxides. The product oxides revert back to the LDH upon soaking in water on account of the compositional and morphological metastability of the former. This is in contrast with the phosphate-intercalated LDHs, in which the reversibility is suppressed, consequent to the formation of stable metal phosphates.



## 1. Introduction

Arsenic is one of the insidious elements present in natural and waste waters, and its toxicity and impact on human health is well known [1]. Arsenic exists in two stable oxidation states, namely As(III) and As(V). The dominant species varies with the pH of the solution. Under oxidative conditions, As(V) exists in four forms in aqueous solution, namely $H_3AsO_4$, $H_2AsO_4^-$, $HAsO_4^{2-}$, and $AsO_4^{3-}$. There is considerable interest in developing new materials to mineralize arsenates effectively.

Layered double hydroxides (LDHs) are widely used for catalysis and sorption and are sinks for the mineralization of insidious anions such as chromates [2,3], selenates [4], fluorides [5], radioactive anions [6], and various organic pollutants [7]. LDHs exhibit anion exchange properties, which make them candidate materials for the immobilization of arsenate in the interlayer region of the LDHs.

The structure of the LDHs is derived from that of the mineral brucite [8]. Brucite comprises a close packing of hydroxyl ions in which $Mg^{2+}$ ions occupy alternative layers of octahedral sites, leading to a stacking of charge-neutral metal hydroxide layers of composition $[Mg(OH)_2]$. When a fraction $x$ of $Mg^{2+}$ ions is replaced by a trivalent ion such as $Al^{3+}$ or $Fe^{3+}$, the positive charge, $x+$, generated on the metal hydroxide layer is compensated for by the inclusion of hydrated anions, $A^{n-}$, in the interlayer region to give LDHs of composition $[M^{II}_{1-x}M'^{III}_x(OH)_2](A^{n-})_{x/n}\cdot mH_2O$, where $M^{II}$ = Mg, Ca, Co, Ni, Zn; $M'^{III}$ = Al, Cr, Fe; and $0.2 \leqslant x \leqslant 0.33$. We refer to the LDH composition by the symbol M/M′-$(A)_x$. In structure and function, the LDHs are anionic clays.

However, the utilization of LDHs in anion amelioration is plagued by several limitations.

1. The LDHs have a solution chemistry in that their solubilities are higher than those of the silica-based cationic clays. There is evidence to show that anion exchange takes place by dissolution and reprecipitation [9]. Anion exchange does not take place unless the LDH of the incoming anion is less soluble than that of the outgoing anion.
2. The reactivity of the LDH is governed in part by the nature of the intercalated anion. Anions contribute to the thermodynamic stability of the LDH by affecting both enthalpy and entropy [10]. For a given pair of metal ions, the affinity of the LDH for different anions varies in the order $CO_3^{2-} > SO_4^{2-} > Cl^- > NO_3^- \gg I^-$ [11]. Therefore, $CO_3^{2-}$-LDHs do not undergo anion exchange. At the other end of the series, $I^-$ cannot be effectively mineralized by LDHs.
3. The affinity for different anions also has a crystal chemical basis. Anions such as $CO_3^{2-}$ ($D_{3h}$) and $SO_4^{2-}$ ($T_d$) possess a symmetry that is compatible with the local symmetry of the interlayer sites in the LDH structure. This symmetry compatibility enhances the H-bonding between the metal-hydroxide

* Corresponding author. Fax: +91 80 22961354.
*E-mail address:* vishnukamath8@hotmail.com (P.V. Kamath).

0021-9797/$ – see front matter 
doi:10.1016/j.jcis.2008.11.054

layers and the interlayer, thereby increasing the affinity of the LDHs for these anions.

The $PO_4^{3-}$ and $AsO_4^{3-}$ ions are both deleterious to the environment. Being ions of tetrahedral symmetry, they can in principle be mineralized in LDHs, in much the same way that $SO_4^{2-}$ ions yield LDHs. Despite this, there are only a few studies of $TO_4^{3-}$ (T = P, As)-containing LDHs, and these anions do not find a place in the affinity series.

There are many reasons for this paucity of work on $TO_4^{3-}$-LDHs.

1. Binary phosphates of divalent as well as trivalent metals are highly insoluble and therefore thermodynamically more stable than LDHs. Consequently coprecipitation reactions yield binary phosphates, rather than $PO_4^{3-}$-LDHs [9,12].
2. The synthesis of $PO_4^{3-}$-LDHs by anion exchange has not been unequivocally established. While Ooi and co-workers [13] report the formation of Mg/Al-$PO_4$ LDHs as a result of $PO_4^{3-}$ uptake by Mg/Al-Cl LDHs, other authors report the formation of binary phosphates under conditions employed to affect anion exchange [11].
3. Binary arsenates have higher solubilities than their carbonate counterparts, on account of which $AsO_4^{3-}$-LDHs are expected to be thermodynamically less stable than LDHs comprising other anions.

Therefore $AsO_4^{3-}$ uptake by LDHs has been studied by (a) discharge of $CO_3^{2-}$ ions by a mineral acid (HCl or $HNO_3$) at pH $\leqslant$ 4.5 [14] and (b) calcination of the pristine LDH to yield a defect oxide phase and subsequent reconstruction of the LDH by soaking the oxide residue in As(V) solution [15]. The uptake by the former method is essentially through anion exchange at a pH close to the dissolution pH of the LDH, while the latter is based on the memory-effect of LDHs.

However, there are few reports on the characterization of arsenate-containing LDHs, which are the final products of As scavenging. Arsenic forms several stable binary arsenates with metal ions. Formation of such binary phases either during synthesis of the LDH or during postsynthesis work-up leads to arsenic speciation that significantly affects its mobility and hence its toxicity. Therefore synthesis and characterization of the arsenate-LDHs is important to (a) quantify the limitations arising from the solution chemistry of LDHs and (b) assess the parameters and conditions that stabilize the arsenate ion in the interlayer.

In this paper, we report structural and compositional features of LDHs intercalated with arsenate ions. Arsenate-intercalated LDHs are synthesized by coprecipitation and by anion exchange reactions. Arsenate exchange at different pH values is also reported. As the aqueous chemistry of arsenates is similar to that of phosphates, pertinent comparisons of the two LDHs are made.

## 2. Materials and methods

### 2.1. Synthesis of LDHs

All reagents were of analytical grade (Merck, India) and were used without further purification. The M/M′-$(A)_{0.33}$ LDHs (M = Mg, Zn, Ni, and Co; M′ = Al; A = $AsO_4^{3-}$, $PO_4^{3-}$, $NO_3^-$) were prepared by the dropwise addition (3 ml $min^{-1}$) of a mixed metal salt solution [$M(NO_3)_2 + Al(NO_3)_3$] into a reservoir containing 10 times the stoichiometric requirement of $A^{n-}$ ions, taken as their sodium salt. A quantity of 2 mol/L NaOH was dispensed using a Metrohm Model 718 STAT Titrino to maintain a constant pH at precipitation (see Table 1). The pH value was chosen based on the formation pH of each individual LDH. $N_2$ gas was bubbled through the solution during precipitation and aging (18 h, 65 °C). The precipitate was rapidly filtered under suction and washed with deionized (15 MΩ cm specific resistance, Millipore Model Elix 3 ion exchange system) decarbonated water and then dried at 65 °C for 24 h.

**Table 1**
Results of coprecipitation reactions in presence of phosphate and arsenate anions.

| Desired LDH | pH of precipitation | Products obtained |
|---|---|---|
| Mg/Al-$AsO_4$ | 10.0 | Mg/Al-$AsO_4$ LDH |
| Zn/Al-$AsO_4$ | 8.5 | $ZnHAsO_4{\cdot}3H_2O + ZnO$ |
| Zn/Cr-$AsO_4$ | 8.0 | $ZnHAsO_4{\cdot}3H_2O + ZnO$ |
| Ni/Al-$AsO_4$ | 7.0 | $NiHAsO_4{\cdot}3H_2O$ |
| Co/Al-$AsO_4$ | 8.5 | X-ray amorphous product |
| Ca/Al-$AsO_4$ | 11.5 | $Ca(OH)_2 + CaAsO_4$ |
| Mg/Al-$PO_4$ | 10.0 | X-ray amorphous product |
| Zn/Al-$PO_4$ | 8.5 | $ZnHPO_4{\cdot}4H_2O + ZnO$ |
| Zn/Cr-$PO_4$ | 8.0 | $ZnHAsO_4{\cdot}4H_2O + ZnO$ |
| Ni/Al-$PO_4$ | 7.0 | $NiHPO_4{\cdot}4H_2O$ |
| Co/Al-$PO_4$ | 8.5 | X-ray amorphous product |
| Ca/Al-$PO_4$ | 11.5 | $CaHPO_4{\cdot}2H_2O$ |

Hydrothermal treatment of the dried powder sample was carried out in deionized, decarbonated water in a Teflon-lined autoclave (150 ml, 50% filling) under autogenous pressure at 140 °C for 18 h. Thermal decomposition was carried out in a silica crucible by heating approximately 350 mg of the sample in a muffle furnace at 800 °C for 18 h. The oxide residues were then furnace-cooled and analyzed by PXRD and IR spectroscopy.

In the case of the Mg/Al-$AsO_4$ LDH, preweighed quantities of the oxide residue were soaked in water for 24 h to study the reversible thermal behavior. The solid was then recovered by filtration through a sintered glass crucible and weighed again to monitor the mass gain.

### 2.2. Characterization

All samples were characterized by powder X-ray diffraction using a Bruker D8 Advance diffractometer (Cu$K\alpha$ source, $\lambda$ = 1.541 Å). Data were collected at a continuous scan rate of 1° $2\theta$ per minute or less and were then rebinned into $2\theta$ steps of 0.02°. IR spectra were recorded using a Nicolet Model Impact 400D FTIR spectrometer (4000–400 $cm^{-1}$, resolution 4 $cm^{-1}$, KBr pellet). Thermal analysis (TG/DTG) studies were carried out using a Mettler-Toledo 851$^e$ TG/SDTA system driven by Star$^e$ 7.1 software (heating rate 5 °C $min^{-1}$, $N_2$ gas). The samples were first heated to 100 °C in the TG balance for 0.5 h to drive away the adsorbed water and then ramped up to 800 °C. The arsenate present in the LDH was estimated by dissolving a preweighed (0.2-g) quantity of the sample in acid (1 ml of concentrated $HNO_3$) and the arsenate concentration in the solution was determined by the silver arsenate method [16].

### 2.3. Arsenate exchange

Preweighed (0.20-g) batches of the Mg/Al-$(NO_3)_{0.33}$ LDHs were suspended in 30 ml of $Na_2HAsO_4{\cdot}7H_2O$ solution containing 10 times the stoichiometric requirement of arsenate ions required to affect a complete exchange of the anions in the pristine LDH. After equilibration, the solid was separated by centrifugation and washed with deionized, decarbonated water. The arsenate concentration in the centrifugate was determined by the silver arsenate method as described elsewhere [16]. The arsenate uptake by the LDHs was calculated from the difference in the initial and final arsenate concentrations and is reported in mmol of arsenate exchanged per gram of LDH taken. The arsenate uptake observed in these experiments is referred to as the arsenate carrying capacity and is compared with the theoretical exchange capacity computed from the molecular formula.

The exchange reactions were also carried out at different pH values. The desired pH was achieved by the addition of 0.1 mol/L $HNO_3$ to the LDH slurry. In any case, the volume of acid added did not exceed 2% of the total volume.

## 3. Results and discussion

### 3.1. Formation of As(V) LDHs

Under oxidizing equilibrium conditions, arsenate and phosphate are present as species of similar charge and structure. The solubility of arsenate (phosphate) salts depends upon the type of cation. While alkali metal arsenates (phosphates) are highly soluble, alkaline earth and transition metal arsenates (phosphates) are insoluble [17]. Table 1 lists the products of coprecipitation reactions in the presence of arsenate (phosphate) anions. Except for the Mg/Al-$AsO_4$ system, the products of the reactions in all other cases were the binary metal arsenates (phosphates). This observation reiterates that the formation of LDHs from solution is governed by thermodynamic factors, which are driven by the solubility of the binary salts relative to the product LDH [18]. Therefore if the divalent metal arsenates (phosphates) are more insoluble than the product LDH, precipitation of the former takes place in preference to the latter.

The PXRD pattern of the Mg/Al-$AsO_4$ LDH obtained by coprecipitation at pH 10 (Fig. 1a) shows a low-angle reflection appearing at $2\theta = 10.9°$ (8.12 Å) followed by another at $2\theta = 23.0°$ (3.87 Å), typical of LDHs. The pattern could be indexed to a hexagonal cell ($a = 3.028$ Å and $c = 24.36$ Å). For a typical LDH crystallizing in the structure of the $3R_1$ polytype, the following Bragg reflections are expected:

1. 00*l* comprising the 003 and 006 reflections;
2. 0*kl* comprising $k = 1$, $l = 2$, 5, and 8 reflections;
3. *hk*0/*hkl* comprising the 110/113 reflections.

In contrast, the PXRD pattern of Mg/Al-$AsO_4$ LDH is characterized by only four broad and asymmetric peaks indicative of structural disorder [19]. Different kinds of disorder account for the asymmetric broadening of the reflections: (i) interstratification broadens the 00*l* reflections while (ii) stacking disorders and turbostraticity account for the extinction of the 0*kl* and *hkl* reflections, respectively. The loss of 3-D periodicity leads to 2-D Bragg reflections that exhibit Warren broadening [20]. No ordering is observed on hydrothermal treatment (Fig. 1b).

Within the interlayer of the LDHs, the anions and water molecules possess high translational and orientational degrees of freedom. From a crystal chemical viewpoint, differences in the coordination symmetry of the anions and the local symmetry of the interlayer site lead to stacking disorders. As a result, the stacking of the rigid metal hydroxide layers is affected significantly by the nonrigid interlayer. Therefore, knowledge of the coordination symmetry of the intercalated anion is crucial for understanding the bonding within the interlayer. This is obtained from IR spectroscopy.

### 3.2. Infrared spectra

The speciation of As(V) is known to vary with pH, with the neutral $H_3AsO_4$ dominant at acidic pH (pH 1 to 4.5), $H_2AsO_4^-$ dominant under mildly acidic conditions (pH 4.5 to 6.5), $HAsO_4^{2-}$ at pH 6.5 to 11.0, and $AsO_4^{3-}$ dominant under highly basic conditions. The ionic radii of the As(V) species expectedly varies with pH in the decreasing order $H_2AsO_4^- > HAsO_4^{2-} > AsO_4^{3-}$.

The tetrahedral $AsO_4^{3-}$ ion has two IR active modes, the triply degenerate antisymmetric stretch ($\nu_3$) and symmetric bend ($\nu_4$)

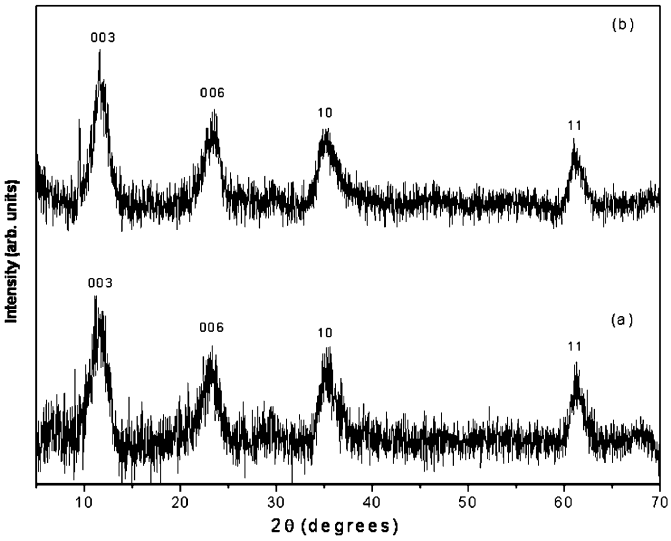


**Fig. 1.** PXRD patterns of (a) as-prepared and (b) hydrothermally treated Mg/Al-$AsO_4$ LDH.

observed at 878 and 463 $cm^{-1}$, respectively [21]. Of these, the latter overlaps with the lattice vibrations of the LDH and cannot be distinguished. When the orthoarsenate ion is protonated, the following changes are expected in the infrared spectrum.

1. For the case of $HAsO_4^{2-}$, the symmetry is reduced to $C_{3v}$. Therefore the triply degenerate $\nu_3$ and $\nu_4$ modes ($F_2$) are split into $A_1$ and $E$, modes increasing the infrared-active vibrations to 6.
2. For the case of $H_2AsO_4^-$, the symmetry is lowered to $C_{2v}$. The doubly degenerate $E$ mode is split into $B_1$ and $B_2$ modes for $\nu_3$ and $\nu_4$, while the $\nu_2$ mode is split into $A_1$ and $A_2$ modes. This increases the infrared-active vibrations to nine.
3. These new vibrations correspond to the As–OH stretching modes (expected between 2400 and 2730 $cm^{-1}$) and deformation modes (1265–1680 $cm^{-1}$).

The magnitude of the splitting reflects the strength of interaction of intercalated $HAsO_4^{2-}$ or $H_2AsO_4^-$ ion with the metal hydroxide layers. In the case of sulfate-intercalated LDHs, the $SO_4^{2-}$ ion is intercalated with one of the S–O bonds parallel to the $c$ crystallographic axis. The basal oxygen atoms and the oxygen of the intercalated water share a single set of sites, while the apical oxygen atom occupies a crystallographically distinct site in the interlayer [22]. This enables the basal O atoms of the $SO_4^{2-}$ ion to participate extensively in H-bonding with the metal hydroxide layers, while the apical oxygen does not participate in any hydrogen bonding [23]. Therefore with lowering of symmetry from $T_d$ to $C_{3v}$ (or $C_{2v}$), the splitting of the degenerate vibration modes is observed [24].

The IR spectrum of Mg/Al-$AsO_4$ LDH (Fig. 2) exhibits a single band at 836 $cm^{-1}$. This corresponds to the triply degenerate asymmetric stretch ($\nu_3$), which in the free orthoarsenate ion appears at 878 $cm^{-1}$. This suggests that the intercalated species is the tetrahedral orthoarsenate anion $AsO_4^{3-}$. The fact that the symmetry of the orthoarsenate ion is not lowered shows that either (i) the interaction with the metal hydroxide layer is weak or (ii) poor structural order causes the interaction to average out, leaving the coordination symmetry unchanged.

Wet chemical analysis yields an arsenate content of 0.09 mol per formula unit as opposed to the expected 0.11 mol per formula unit.

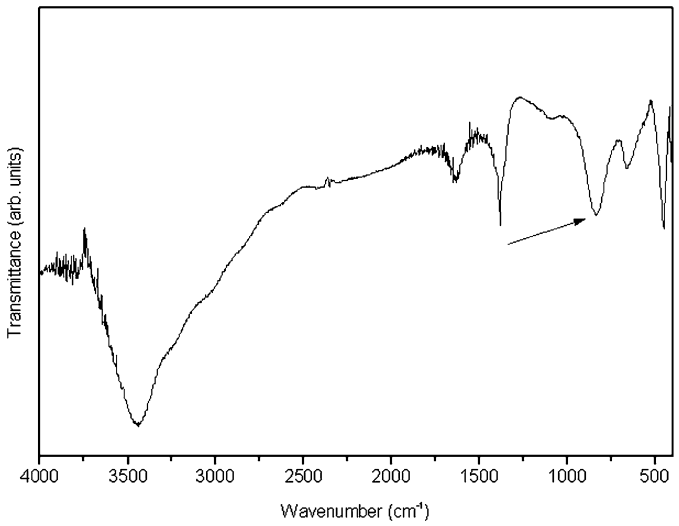


**Fig. 2.** Infrared spectra of as-prepared Mg/Al-$AsO_4$ LDH. The arrow indicates the position of the $\nu_3$ mode of $AsO_4^{3-}$.

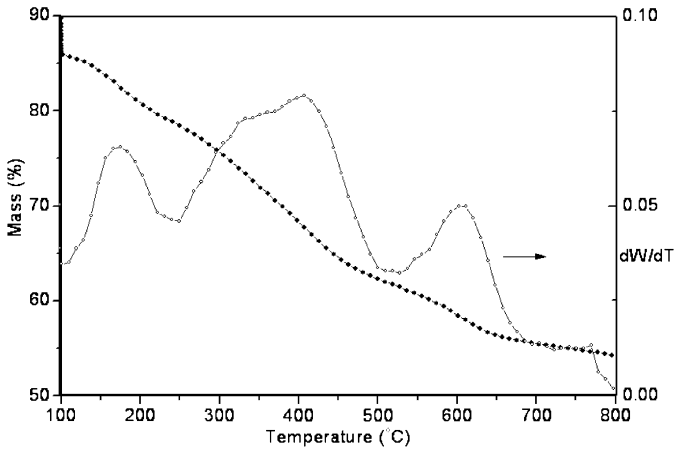


**Fig. 3.** TG profile of the Mg/Al-$AsO_4$ LDH.

### 3.3. Thermal behavior of As(V) LDHs

The TG/DTG profile of the Mg/Al-$AsO_4$ LDH (Fig. 3) can be explained by the following steps:

Step 1: $Mg_6Al_3(OH)_{18}(AsO_4)\cdot 4.5H_2O \rightarrow$

$$Mg_6Al_3(OH)_{18}(AsO_4) + 4.5H_2O,$$

Step 2: $Mg_6Al_3(OH)_{18}(AsO_4) \rightarrow$

$$1.5MgAl_2O_4 + 0.167As_6O_{11}\cdot H_2O + 4.5MgO.$$

The mass loss below 100 °C can be attributed to the loss of adsorbed water. The mass loss between 100 and 800 °C amounts to 38.7% (against the theoretically expected value of 33.7%). Loss of mass as volatile gas renders the end product of the decomposition reaction microporous, with the incomplete tail of the TGA profile signifying the loss of the volatile gas through such micropores [25].

The absence of basal reflections in the PXRD pattern of the product (Fig. 4a) of decomposition of Mg/Al-$AsO_4$ LDH (600 °C) indicates the collapse of the layered structure. The broad feature in the mid-2$\theta$ region (30°–45° 2$\theta$) signifies the formation of poorly crystalline periclase. The PXRD pattern of the product obtained by soaking the above oxide residue in water (Fig. 4b) shows that the layered phase is reconstructed as signified by the reappearance of the basal reflection at 11.8° 2$\theta$ (7.5 Å). The oxide residue regains

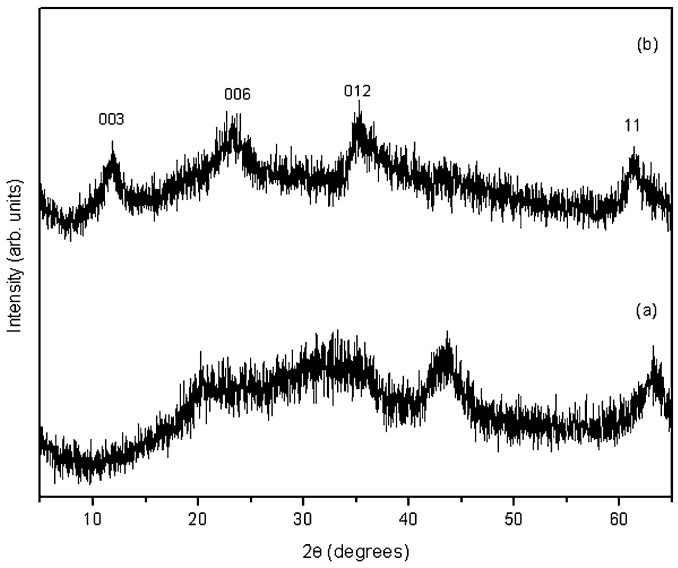


**Fig. 4.** PXRD patterns of (a) freshly calcined (600 °C) oxide residue of the Mg/Al-$AsO_4$ LDH and (b) LDH obtained by soaking (a) in water.

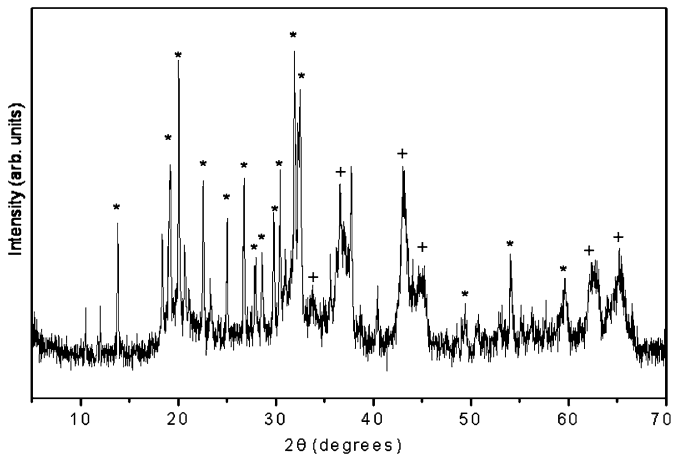


**Fig. 5.** PXRD pattern of the residue obtained after thermal decomposition of Mg/Al-$AsO_4$ LDH at 800 °C. Features marked ∗ and + correspond to $2As_2O_3\cdot As_2O_5\cdot H_2O$ and MgO phases, respectively.

16% of its original mass to yield an LDH. This is in direct contrast with the thermal behavior of phosphate-intercalated LDHs, where the reversible behavior is suppressed [26].

The reversibility of $AsO_4^{3-}$-intercalated LDHs can be explained on the basis of the products formed upon thermal decomposition. Unlike $CO_3^{2-}$, $NO_3^-$, $Cl^-$, or $SO_4^{2-}$ ions, the intercalated $AsO_4^{3-}$ is nonvolatile. To identify the products of thermal decomposition of the Mg/Al-$AsO_4$ LDH, the oxide residue shown in Fig. 4a was sintered at 800 °C (Fig. 5). The oxide residue comprises a poorly crystalline periclase (MgO) phase and $As_6O_{11}\cdot H_2O$. The latter is a mixture of As(V) and As(III) oxides ($2As_2O_3\cdot As_2O_5\cdot H_2O$, JCPDS PDF No. 22-1050). The reversible thermal behavior of LDHs is driven by the compositional and morphological metastability of this mixed oxide phase [26]. It is well documented that the reconstruction of the layered phase and the formation of thermodynamically stable spinel are competing reactions. The reversibility is suppressed in the case of phosphate-intercalated LDH by the formation of magnesium phosphate, in which the $Mg^{2+}$ ions share identical octahedral coordination, as in the thermodynamically stable spinel phase. The situation is radically different in the arsenate-intercalated LDHs, where the intercalated arsenate ion partially undergoes reductive deintercalation to form a mixture of As(III) and

As(V) oxides, along with the defect rock salt phase. Upon soaking in water, the As(V) species is preferentially intercalated into the interlayer, while the more soluble As(III) oxide is washed off during postsynthesis modifications. This also explains the partial reversibility.

It is to be noted that upon heating, there is a change in speciation of arsenic as the $AsO_4^{3-}$ ion undergoes reduction at high temperatures to yield As(III) species. This is significant in the context of As remediation because the As(III) species is orders of magnitude more soluble than As(V) and hence more toxic. Therefore thermal treatments of arsenate-intercalated LDHs to immobilize arsenate are inherently ineffective. This is in direct contrast to amelioration of other anions by LDHs, such as chromate, where upon thermal treatment the deleterious Cr(VI) is immobilized efficiently as Cr(III) oxide, embedded in the matrix of the thermodynamically stable spinel [27].

### 3.4. Arsenate exchange characteristics

#### 3.4.1. Mechanism of exchange

With the coprecipitation of metal salts with arsenate or phosphate yielding the more insoluble and thermodynamically stable unitary phases, anion exchange reactions offer a simple soft-chemistry route to synthesize metastable arsenate- or phosphate-intercalated LDHs. The mechanism of anion-exchange reactions varies with the choice of the pristine LDH, the nature of the intercalated anion, and the solubility of the product LDH. Accordingly, the LDH of Ca with Al due to its higher solubility predominantly undergoes anion exchange through a dissolution–reprecipitation mechanism, while the anion exchange reactions of Ni-Al LDH progress topotactically.

To illustrate the plausible mechanism of anion exchange and reflect upon the relative stability of the intermediate phases, if any, two related phases, $Mg(OH)_2$ and $Al(OH)_3$, were aged in arsenate solution at the natural pH of the latter (pH 8.5) as controls. Both these compounds compose charge-neutral layers and do not posses any interlayer chemistry. The results are shown in Fig. 6. While $Al(OH)_3$ remains unchanged, $Mg(OH)_2$ transforms to $MgHAsO_4$. This suggests that there is a dissolution of $Mg(OH)_2$ followed by the precipitation of a binary arsenate. Therefore if the anion-exchange reactions involving arsenate ions proceed through the dissolution–reprecipitation mechanism, magnesium arsenate is expected to form at the expense of arsenate-intercalated LDH.

The PXRD patterns of Mg/Al-$(NO_3)_{0.33}$ LDH and the product obtained after arsenate exchange are shown in Fig. 7. The PXRD pattern of the product shows all features attributable to a layered phase. There is a decrease in the basal distance from 8.89 Å (9.9° $2\theta$) to 8.43 Å (10.5° $2\theta$) after exchange, indicating the incorporation of arsenate species into the interlayer of the LDH. The IR spectra of the product (data not shown) show that the $\nu_3$ mode of $NO_3^-$ at 1383 $cm^{-1}$ is completely extinguished and new absorptions arise around 840 $cm^{-1}$. The latter can be attributed to the intercalated arsenate species. The PXRD pattern is devoid of any secondary phases. The relative ease of exchange of $NO_3^-$ for arsenate and the formation of arsenate-intercalated LDHs indicate that the exchange reactions take place topotactically. In comparison with the LDH obtained by coprecipitation, the arsenate LDH obtained by anion exchange is better ordered and retains all the features of the precursor $NO_3^-$-LDH, as would be expected of a reaction following the topotactic mechanism [24]. Table 2 lists the results of arsenate-exchange reactions of various LDHs.

#### 3.4.2. Effect of pH

As the anion-exchange reactions are driven by the relative solubilities of the pristine as well as the product LDHs, pH plays a significant role in the energetic and mechanistic aspects of these

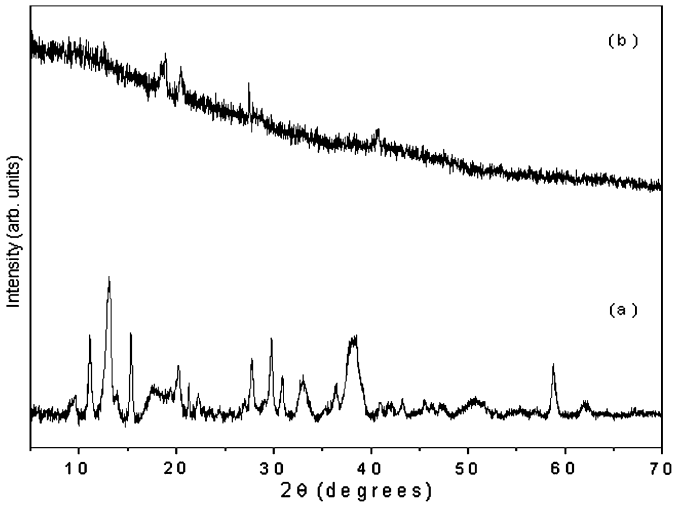


**Fig. 6.** PXRD patterns of the products obtained by aging (a) $Mg(OH)_2$ and (b) $Al(OH)_3$ in a $Na_2HAsO_4{\cdot}7H_2O$ solution.

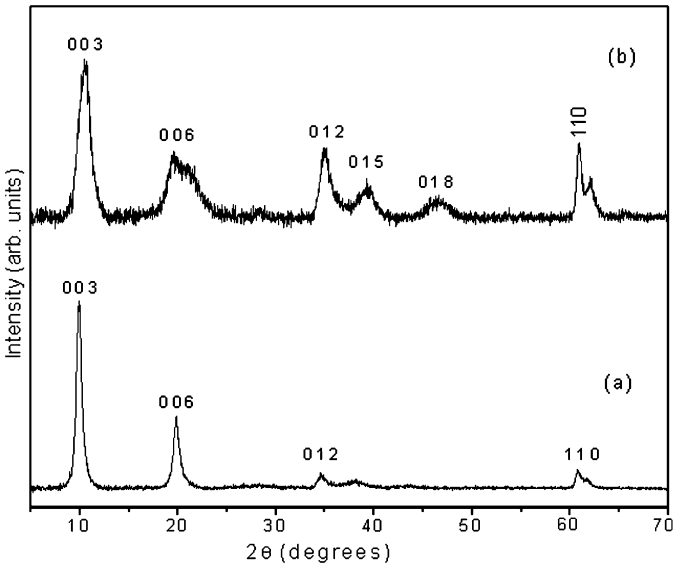


**Fig. 7.** PXRD patterns of (a) Mg/Al-$(NO_3)_{0.33}$LDH and (b) product obtained after arsenate exchange.

**Table 2**
Characterization of various arsenate intercalated LDHs obtained by anion exchange reactions.

| LDH | Final pH | Cell parameters | | TG mass loss[a] (%) |
|---|---|---|---|---|
| | | *a* (Å) | *c* (Å) | |
| Mg/Al-$AsO_4$ | 9.2 | 3.040 | 25.294 | 38.7 (33.7) |
| Zn/Al-$AsO_4$ | 8.3 | 3.071 | 25.250 | 27.2 (25.4) |
| Zn/Cr-$AsO_4$ | 7.8 | 3.104 | 23.827 | 25.2 (23.6) |
| Ni/Al-$AsO_4$ | 7.7 | 3.041 | 24.360 | 28.9 (26.5) |
| Co/Al-$AsO_4$ | 8.1 | 3.070 | 23.110 | 31.3 (24.0) |

[a] Values in parentheses are the expected mass losses.

reactions. Fig. 8 shows the effect of pH on the basal distance and the arsenate carrying capacity of Mg/Al-$(NO_3)_{0.33}$ LDH. At low pH values (pH < 6), the Mg–Al LDH is expected to undergo severe dissolution, resulting in the formation of the $MgHAsO_4$ phase.

At near-neutral and neutral pH values, $H_2AsO_4^-$ and $HAsO_4^{2-}$ species are in equilibrium with each other, with the latter slightly in excess. The $HAsO_4^{2-}$ species, being divalent, can be thought of as preferentially exchanging for nitrate, even though a small amount of $H_2AsO_4^-$ incorporation cannot be ruled out. The basal distance

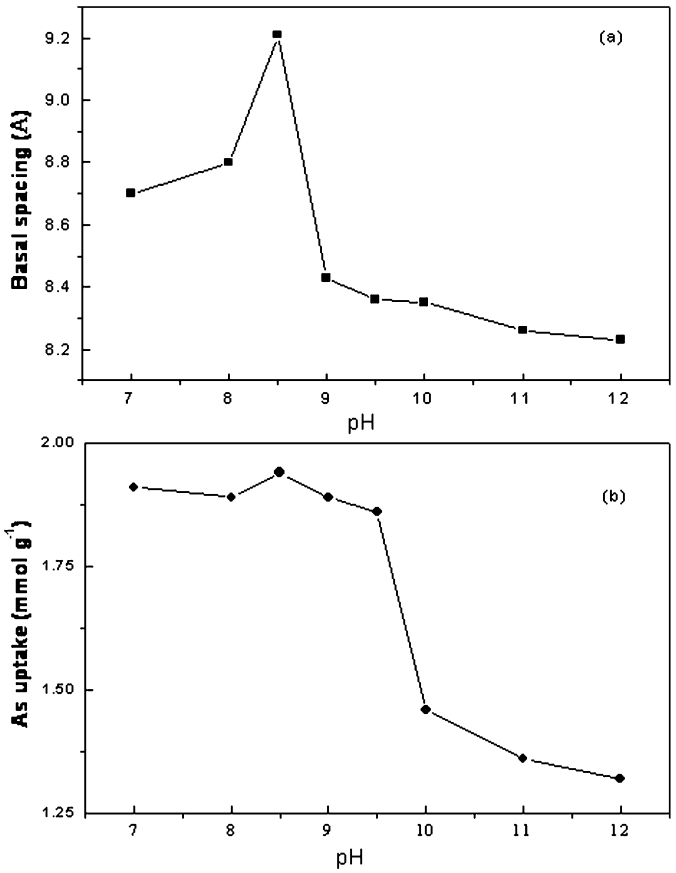


**Fig. 8.** Effect of pH on (a) basal distance of arsenate LDHs and (b) arsenate carrying capacity.

of 8.7 Å observed at these pH values can be thought of an intermediate value, obtained by possible interstratification of the two arsenic species in the interlayer. The broader 006 reflection in the PXRD pattern corroborates this observation (see Fig. 7b).

At pH values greater than 8, the $HAsO_4^{2-}$ ion predominates. Subsequently, there is an increase in the basal distance to 9.2 Å due to the incorporation of the larger $HAsO_4^{2-}$ ion. The arsenate carrying capacity also increases to 1.94 mmol $g^{-1}$ of LDH, closer to the theoretically expected value of 1.96 mmol $g^{-1}$ of LDH calculated for the $HAsO_4^{2-}$ ion. As the pH is further increased, the trivalent orthoarsenate $AsO_4^{3-}$ species dominates. This is reflected in a decrease in the basal distance of the exchanged product at high pH due to the incorporation of the smaller $AsO_4^{3-}$ ion. The arsenate carrying capacity also falls to 1.32 mmol $g^{-1}$, as only one $AsO_4^{3-}$ ion can be exchanged for three $NO_3^-$ ions.

### 3.4.3. Effect of equilibration time

It is well established that the anion-exchange reactions are extremely fast, and the exchange kinetics are studied by T-jump techniques [28]. Nonetheless, the effect of aging time on the structure of the arsenate-intercalated LDHs is necessary to gain an insight into the stability of the immobilized arsenate. Table 3 lists the results of varying the equilibration time. In keeping with our earlier observations [3], equilibration time does not have a significant effect on the arsenate carrying capacity. The basal distance also does not vary appreciably. This observation is in direct contrast with the phosphate-containing LDHs, which show substantial variation in the basal distance with equilibration time, as noted elsewhere [29]. These results point out that the interlayer regions of arsenic-containing LDHs are less flexible than with sulfate- or phosphate-intercalated LDHs, paving the way for effective immobilization of arsenic.

**Table 3**
Effect of equilibration time and pH on arsenate and phosphate exchange.

| Phosphate exchange | | | Arsenate exchange | | |
|---|---|---|---|---|---|
| Equilibration time (h) | pH | Interlayer spacing (Å) | Equilibration time (h) | pH | Interlayer spacing (Å) |
| 1 | 7.5 | 8.62 | 1 | 9.2 | 8.36 |
| 5 | 7.5 | 9.14 | 5 | 9.2 | 8.43 |
| 5 | 9.4 | 9.97 | 24 | 9.2 | 8.39 |
| 24 | 9.4 | 8.72 | 5 | 7 | 8.71 |
| 5 | 7 | 9.06 | 5 | 8 | 8.82 |
| 5 | 8 | 9.14 | 5 | 8.5 | 9.21 |
| 5 | 9 | 9.96 | 5 | 9 | 8.43 |
| 5 | 10 | 8.97 | 5 | 10 | 8.35 |
| 5 | 11 | 8.87 | 5 | 11 | 8.26 |
| 5 | 12 | 8.22 | 5 | 12 | 8.23 |

## 4. Summary

In conclusion, immobilization of arsenate by LDHs through anion-exchange reactions offers an efficient means to mineralize insidious As(V). The arsenate exchange strongly correlates with the pH of the solution. The thermal behavior and solution chemistries of arsenate LDHs are different from those of the phosphate-intercalated LDHs, with the former having a less flexible interlayer, paving the way for sequestration of As(V).

## Acknowledgments

The authors thank the Department of Science and Technology (DST), Government of India (GOI), for financial support. P.V.K. is a recipient of the Ramanna Fellowship of the DST. S.V.P. thanks the Council of Scientific and Industrial Research (CSIR) for the award of a Senior Research Fellowship.

## References

[1] D.V. Vaughan, Elements 2 (2006) 71–75.
[2] S.V. Prasanna, R.A.P. Rao, P.V. Kamath, J. Colloid Interface Sci. 304 (2006) 292.
[3] S.V. Prasanna, P.V. Kamath, Solid State Sci. 10 (2008) 260.
[4] Y. You, G.F. Vance, H. Zhao, Appl. Clay Sci. 20 (2001) 13.
[5] L. Lv, J. He, M. Wei, X. Duan, Ind. Eng. Chem. Res. 45 (2006) 8623.
[6] J. Serrano, V. Bertin, S. Bulbulian, Langmuir 16 (2000) 3355.
[7] M.A. Ulibarri, M.C. Hermosin, in: V. Rives (Ed.), Layered Double Hydroxides: Past and Future, Nova Science, New York, 2001, pp. 251–284.
[8] F. Cavani, F. Trifiro, A. Vaccari, Catal. Today 11 (1991) 173.
[9] A.V. Radha, P.V. Kamath, C. Shivakumara, Solid State Sci. 7 (2005) 1180.
[10] Y. Israeli, C. Taviot-Gueho, J.P. Besse, J.P. Morel, N. Morel-Desrosiers, J. Chem. Soc. Dalton Trans. (2000) 791.
[11] S. Miyata, Clays Clay Miner. 31 (1983) 305.
[12] B. Houri, A. Legrouri, A. Barroug, C. Forano, J.P. Besse, Collect. Czech. Chem. Commun. 63 (1998) 732.
[13] A. Ookubo, K. Ooi, H. Hayashi, Langmuir 9 (1993) 1418.
[14] G. Carja, S. Ratoi, G. Ciobanu, I. Balasanian, Desalination 223 (2008) 243.
[15] L. Yang, M. Dadwhal, Z. Shahrivari, M. Ostwal, P.K.Y. Liu, M. Sahimi, T.T. Tsotsis, Ind. Eng. Chem. Res. 45 (2006) 4742.
[16] J. Bassett, R.C. Denney, G.H. Jeffery, J. Mendham, in: Vogel's Textbook of Quantitative Inorganic Analysis, 4th edition, Longman, 1978, pp. 344–345.
[17] R.C. Weast (Ed.), CRC Handbook of Chemistry and Physics, CRC Press, Florida, 1986–1987, pp. B103–B104.
[18] R.K. Allada, A. Navrotsky, H.T. Berbeco, W.H. Casey, Science 296 (2002) 721.
[19] M. Bellotto, B. Rebours, O. Clause, J. Lynch, D. Bazin, E. Elkaïm, J. Phys. Chem. 100 (1996) 8527.
[20] D.R. Hines, G.T. Seidler, M.M.J. Treacy, S.A. Solin, Solid State Commun. 101 (1997) 835.
[21] K. Nakamoto (Ed.), Infrared and Raman of Inorganic and Coordination Compounds, Wiley, New York, 1986.
[22] T. Witzke, G. Raade, Neus Jahrbuch für Mineralogie Monatshefte, 2000, pp. 455–465, and Inorganic Crystal Structure Database (ICSD) No. CC91860.
[23] A.S. Bookin, V.A. Drits, Clays Clay Miner. 41 (1993) 551.
[24] A.V. Radha, P.V. Kamath, C. Shivakumara, J. Phys. Chem. B 111 (2007) 3411.

[25] A. Delahay-Vidal, K. Tekaia-Elhsissen, P. Genin, M. Figlarz, Eur. J. Solid State Inorg. Chem. 31 (1994) 823.
[26] A.V. Radha, P.V. Kamath, N. Ravishankar, C. Shivakumara, Langmuir 23 (2007) 7700.
[27] S.V. Prasanna, P.V. Kamath, C. Shivakumara, Mater. Res. Bull. 42 (2007) 1028.
[28] N. Mikami, M. Sasaki, S. Horibe, T. Yasunaga, J. Phys. Chem. 88 (1984) 1716.
[29] M. Badreddine, M. Khaldi, A. Legrouri, A. Barroug, M. Chaouch, A. De Roy, J.P. Besse, Mater. Chem. Phys. 52 (1998) 235.